

Implementation of Two Methods for Designing the Profiles of Mirrors in Quasi-Optical Mode Converter for 170 GHz Transverse Output Gyrotron

Guohui Zhao^{1, 2}, Qianzhong Xue^{1, 2, *}, Yong Wang^{1, 2}, Xuewei Wang^{1, 2}, Shan Zhang^{1, 2}, Gaofeng Liu^{1, 2}, and Lianzheng Zhang¹

Abstract—In order to improve the efficiency of the quasi-optical mode converter, two methods to design mirror systems for a 170 GHz gyrotron operating in $TE_{32,9}$ mode are presented in this paper. The first method is to use Katsenelenbaum-Semenov Algorithm (KSA) to design the structure of the mirror. The second method to design the mirror system depends on the phase difference on the mirrors, so we name it PD method. The mirror system consists of three mirrors, and the mirror center position and mirror size are the same for both methods. For the first method, the scalar and vector correlation coefficients obtained at the window are 99.45% and 98.12%, respectively, and the mirror system has been designed with a transmission efficiency of 97.25%. The scalar and vector correlation coefficients and mirror system transmission efficiency are 99.73%, 98.85%, and 97.67% respectively for the second method. Simulation results of the two methods are compared and analyzed, which provide a reference for the design of gyrotron quasi-optical mode converter mirror system.

1. INTRODUCTION

The gyrotron quasi-optical mode converter consists of two components: 1) a launcher which transforms the cavity mode into a Gaussian-like beam; 2) a mirror system which can change the direction and correct the phase of the Gaussian-like beam. The beam mentioned below in this paper refers to Gaussian-like beam (or RF beam). For high power gyrotrons, high efficiency is very important not only to minimize the prime power required for operation but also to guarantee satisfactory operation over the lifespan of the device [1–3]. Improving the efficiency of the quasi-optical mode converter is of great importance. There are two ways to improve the efficiency of quasi-optical mode converter. One is to increase the Gaussian mode content of the beam radiated from the quasi-optical launcher; the other is to improve the transmission efficiency of the mirror system which is directly related to the Gaussian beam content of the output beam on the window. In recent years, with the development of the International Thermonuclear Experimental Reactor (ITER) project, researchers have done a lot of work on the gyrotron quasi-optical mode converter. In [4] the authors proposed a numerical synthesis method to design a hybrid-type launcher for increasing the Gaussian mode content of the radiation beam. A launcher designed by this new method has been tested to transform the $TE_{32,9}$ mode of the ITER EU 1-MW gyrotron operating at 170 GHz. In [5], a quasi-optical mode converter which consists of a Denisov launcher and a quadratic surface mirror system for a 0.42 THz, $TE_{17,4}$ mode pulsed gyrotron has been designed and tested. Since the phase correcting mirror is not designed by the authors, the scalar Gaussian mode content is only 95.2% on the window by hot test. It is necessary to add phase correction mirrors to the mirror system to improve the Gaussian mode content on the window.

Received 3 December 2018, Accepted 7 March 2019, Scheduled 15 April 2019

* Corresponding author: Qianzhong Xue (qianzhong_xue@mail.ie.ac.cn).

¹ Key Laboratory of High Power Microwave Sources and Technologies, Institute of Electronics, Chinese Academy of Sciences, Beijing 101407, China. ² University of Chinese Academy of Sciences, Beijing 101408, China.

In the gyrotron quasi-optical mode converter, the beam radiated from the quasi-optical launcher is an elliptical Gaussian beam with certain astigmatism and ellipticity. Ellipticity is defined as the ratio of the beam waists in perpendicular directions, and astigmatism is defined as the difference of positions of the beam waists [6]. Mirrors with quadratic surface contour functions are widely used to shape the beam radiated from the launcher in order to obtain a Gaussian field distribution with desired parameters at the gyrotron window. When the Gaussian-like beam is incident perpendicularly to these mirrors, it can be converted into another Gaussian-like beam characterized by a different set of parameters. However, in the quasi-optical mode converter mirror system, the wave beam is incident to the mirrors at a certain angle. Then the quadratic surface mirrors do not match the wave-front phase well, which leads to low transmission efficiency of the mirror system [6, 7].

Phase correction is one of the effective ways to improve the Gaussian mode content on the window. Early phase correction mostly relied on beam measurement experiments. In [8, 9], the authors measured the field amplitudes at different positions on the beam propagation path and obtained the mirror profile by phase iteration algorithm. Due to the tedious process of experimental measurement, this method is rarely used at present. KSA is relatively simple and easy to implement. The convergence speed and accuracy of the algorithm can meet the development requirements of high-power gyrotron quasi-optical mode converter [10–13]. In order to improve the Gaussian mode content of the RF beam furthermore, and then to decrease the stray radiation in the tube, two adapted phase correcting mirrors have been designed by KSA for a 170 GHz $TE_{34,19}$ mode coaxial-cavity ITER gyrotron at Karlsruhe Institute of Technology (KIT) [14]. In [15, 16], two adapted phase correcting mirrors have been designed for a 94 GHz TE_{62} mode gyrotron. A new method (PD method in this paper) for synthesis of beam-shaping mirrors is proposed to reduce the astigmatism and ellipticity of the beam further. In [17], PD method was first adopted to design a mirror system for a 1-MW, continuous wave, 170-GHz, $TE_{32,9}$ -mode gyrotron in International Thermonuclear Experimental Reactor (ITER) within the European Gyrotron Consortium. In the published article, the author did not describe how the PD method was implemented, and the results showed that there was a side lobe besides Gaussian field distribution on the window. The key point of PD method is to generate the surface contours of mirrors according to the phase difference distributions between the incident wave beam and required Gaussian beam.

The relative position of the mirrors and coordinate system are shown in Fig. 1. Mirror 1 is an elliptic cylindrical surface mirror which can focus the beam in X direction. For KSA method mirror 2 is a quadratic surface mirror, and mirror 3 is iteratively optimized as adapted phase correcting mirror based on the KSA to transform the outgoing wave beam into a fundamental Gaussian mode. For PD method, the theoretical analysis shows that it requires at least two phase-correcting mirrors to complete the design of the mirror system, so mirror 2 and mirror 3 are both beam-shaping mirrors.

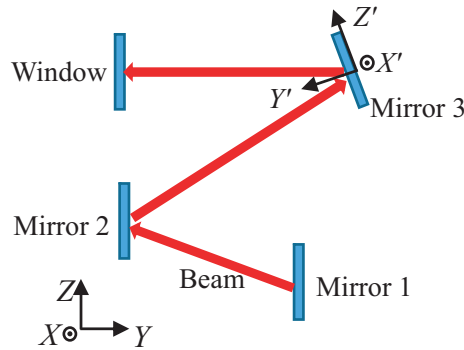


Figure 1. Structure of the mirror system.

This paper is organized as follows. Section 2 shows the radiation field of the launcher. Design of a mirror system based on KSA method is described in Section 3, while Section 4 presents the mirror system designed by PD method. The discussion and conclusion are given in Section 5.

2. RADIATION FIELD OF THE LAUNCHER

The design of the mirror system begins with the analysis of radiation field of the launcher (see Fig. 2 and Fig. 3). In order to avoid the outgoing beam from mirror 1 to be reflected by the launcher, the distance between mirror 1 and the launcher should be larger than 60 mm. The field radiated from the launcher is quite divergent in space, and the ellipticity of the beam is 2.85 at the distance of 60 mm from the launcher aperture, which is difficult to use KSA or PD method to design a well-worked mirror system. It is necessary to focus the beam with an elliptic cylindrical surface mirror before designing the beam-shaping mirrors. The surface of mirror 1 is calculated by Equation (1).

$$Y = -\frac{fe}{2} + \left(\frac{A}{2}\right) \sqrt{1 - \frac{X^2}{(B/2)^2}} \tag{1}$$

where fe is the focal length, and A and B are the long axis and short axis, respectively. $fe/2 = \sqrt{(A/2)^2 - (B/2)^2}$.

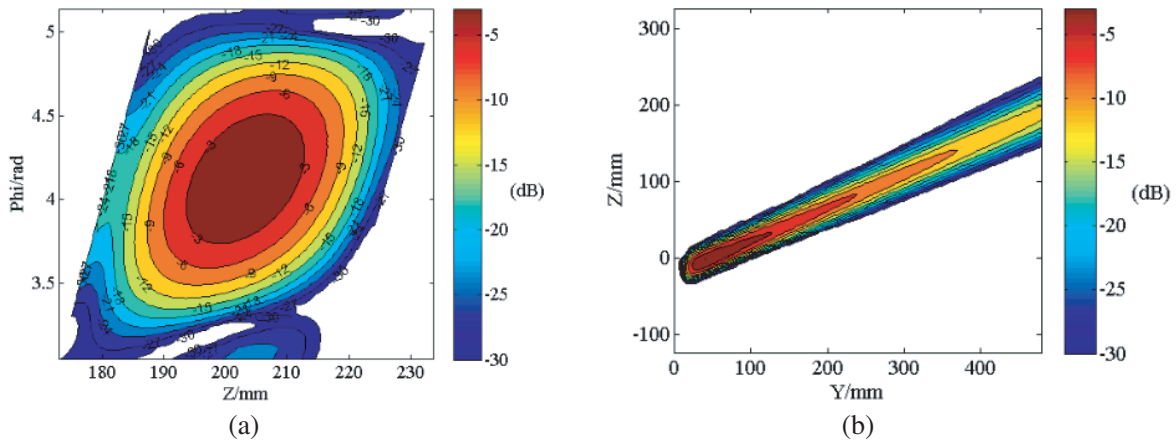


Figure 2. (a) E_x field amplitude (dB) distribution on the aperture, (b) E_x radiation field amplitude (dB) distribution of the launcher in YZ plane.

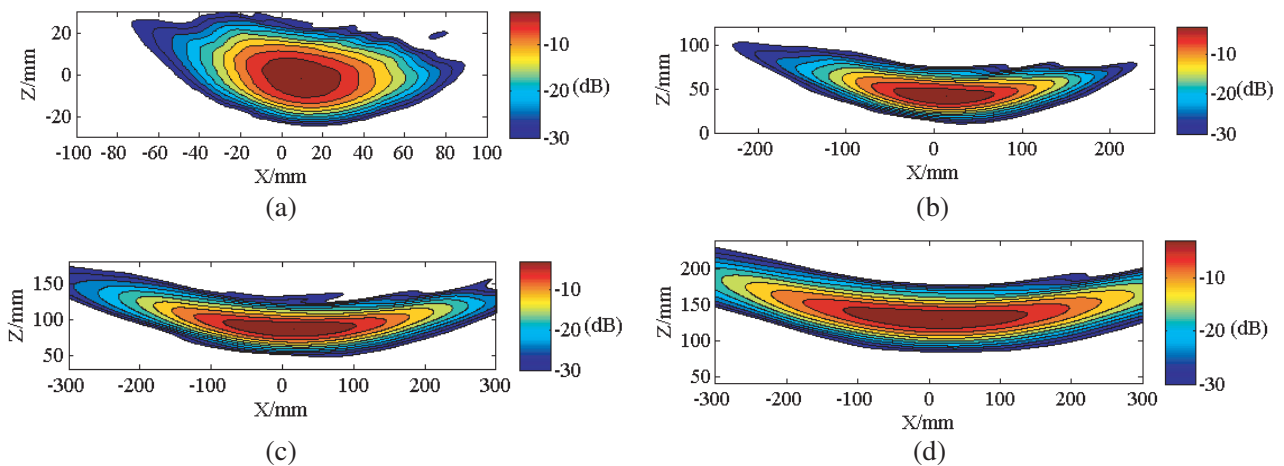


Figure 3. Radiated E_x field amplitude (dB) distribution in the planes at the distance of (a) 50 mm, (b) 150 mm, (c) 250 mm and (d) 350 mm before the launcher.

3. KSA METHOD TO DESIGN MIRROR SYSTEM

The mirror system consists of three mirrors. The first mirror is an elliptic cylindrical surface mirror, and it is used to focus the divergent beams radiated from the launcher. The second mirror which is a bifocal mirror shapes the beam incident on the third mirror. The third mirror is an adapted phase-correcting mirror with a complicated non-quadratic shape function of the surface which is designed to produce the desired beam on the gyrotron output window.

The reflection of the beam on the phase correction mirror is shown in Fig. 4. S' is the area of mirror 3, and S is the area of the window. $u(\vec{r}')$ is an input field on mirror 3. Due to the surface perturbations $\Delta y'$, the phase difference between the input and reflected field is $2k\Delta y' \cos \gamma$, with γ denoting the angle of incidence. There are small altitude changes of the surface on the phase-correcting mirror, which modify the phase of the local plane wave and leave the amplitude of the reflected field at a plane mirror unchanged (see Fig. 4) [13]. The theory of KSA method can be described as follows [14]:

$$\begin{cases} u_c(r') = u(\vec{r}') e^{j2k\Delta y'^i \cos \gamma} \\ u_r(\vec{r}) = 2 \iint_{S'} u_c(r') \frac{\partial G(\vec{r} - \vec{r}')}{\partial y'} dx' dz' \\ q^i(\vec{r}') = -4 \iint_S (u_g(\vec{r}) - u_r^i(\vec{r}))^* \frac{\partial (G(\vec{r} - \vec{r}'))}{\partial y'} dx dz \\ \Delta y'^{i+1} = \frac{1}{2k \cos \gamma} \left[\frac{\pi}{2} - \arg(j2ku(\vec{r}') q^i(\vec{r}') \cos \gamma) \right] \end{cases} \quad (2)$$

where $u_c(r')$ is the reflected field, k the wavenumber in free space of TE_{32,9} mode at 170 GHz, i the iteration number, $q^i(\vec{r}')$ an error function, $u_g(\vec{r})$ the ideal Gaussian field on the window, $\Delta y'^{i+1}$ the surface deformation of phase-correcting mirror generated by adaptive iteration, and $G(\vec{r} - \vec{r}')$ the Green function in free space which can be written as:

$$G(\vec{r} - \vec{r}') = \frac{e^{-jk|\vec{r} - \vec{r}'|}}{4\pi |\vec{r} - \vec{r}'|} \quad (3)$$

The parameters in Equations (2) and (3) with a superscript “ i ” are related to mirror 3, while those without superscript “ i ” are related to the window in this section. From Equation (2), it can be seen that the KSA is an adaptive iterative optimization algorithm. The mirror shaped by KSA can generate arbitrary field distributions theoretically.

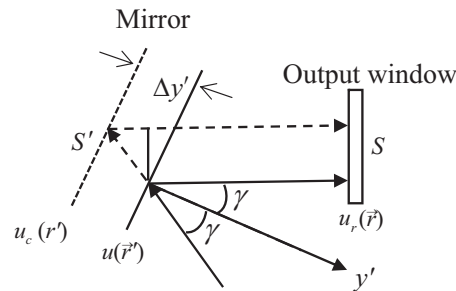


Figure 4. Reflection of a beam on different planes.

The parameters of the mirrors are shown in Table 1. The reference plane of tilt angles θ_x and θ_z is the XZ plane at $Y = 60$ mm for mirror 1. θ_x and θ_z are the rotation angles of the mirror in the X and Z directions, respectively. For mirror 3, the reference plane is the XZ plane at $Y = 100$ mm.

With the phase-correcting mirrors, the beam adjusts its phase distribution to Gaussian beam. To compare the correlation between two beams we usually use correlation coefficient. The scalar correlation coefficient formula which is only related to the amplitude of the two beams can be obtained from

Table 1. Parameters of the mirror system designed by KSA method.

	Mirror center (x, y, z) [mm]	Mirror size (dx, dz) [mm]	Focal length F_x [mm]	Focal length F_z [mm]	Tilt angle θ_x [deg]	Tilt angle θ_z [deg]
M1	(0, 60, 0)	(160, 70)	425	Inf	9.5	0
M2	(0, -330, 171.9)	(150, 150)	-1000	800	0	0
M3	(0, 100, 372.4)	(150, 150)	-	-	0	-11.5
Window	(0, -340, 372.4)	(60, 6)	Inf	Inf	0	0

Equation (4). Equation (5) presents the vector correlation coefficient formula, which shows a relation to both amplitude and phase.

$$\eta_s = \frac{\int_s |u_i| \cdot |u_g| ds \cdot \int_s |u_i| \cdot |u_g| ds}{\int_s |u_i|^2 ds \cdot \int_s |u_g|^2 ds} \tag{4}$$

$$\eta_v = \frac{\int_s |u_i| \cdot |u_g| e^{j(\phi_i - \phi_g)} ds \cdot \int_s |u_i| \cdot |u_g| e^{j(\phi_g - \phi_i)} ds}{\int_s |u_i|^2 ds \cdot \int_s |u_g|^2 ds} \tag{5}$$

In the above equations, u_i is the field calculated numerically, and u_g is the ideal Gaussian field. ϕ_i and ϕ_g are the phases of u_i and u_g , respectively. The beam waist radius of the ideal Gaussian field u_g is 29 mm on the window in this paper.

Figure 5 shows the surface profile of mirror 3, which is $\Delta y'$ in Fig. 4. In Fig. 6, it can be seen that when the iteration number is 20, the scalar correlation coefficient and vector correlation coefficient converge to 99.45% and 98.12%, respectively. The field amplitude (dB) distribution and phase pattern distribution on the window before phase-correcting (see Fig. 7) and after phase-correcting (see Fig. 8) are calculated. The black circle represents the edge of the window with a radius of 60 mm in Fig. 8. In Fig. 8(a), the thick contours are the ideal Gaussian field distribution on the window, and the thin

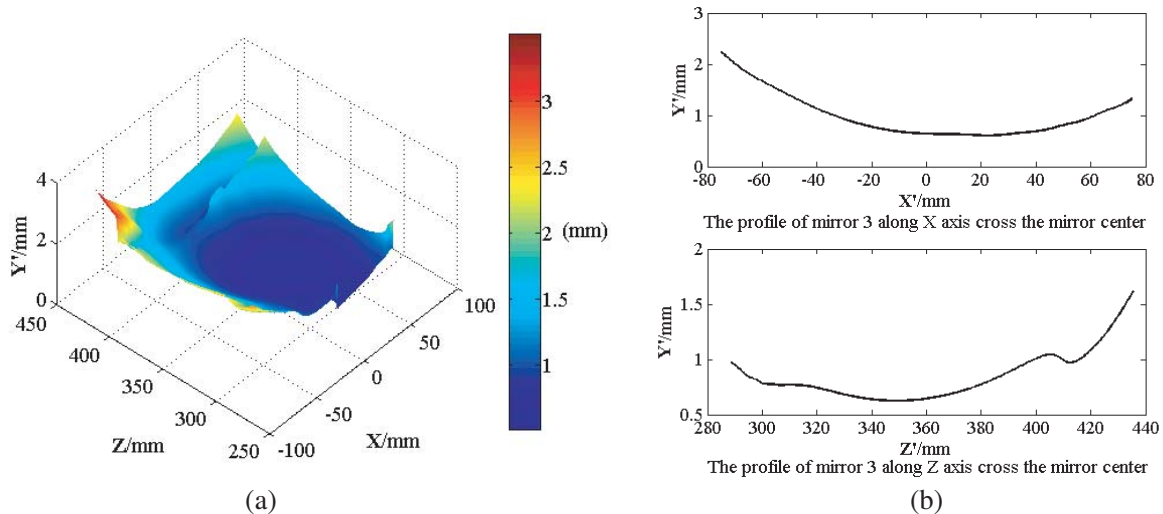


Figure 5. The (a) the surface profile and (b) the section profile of adapted phase-correcting mirror 3.

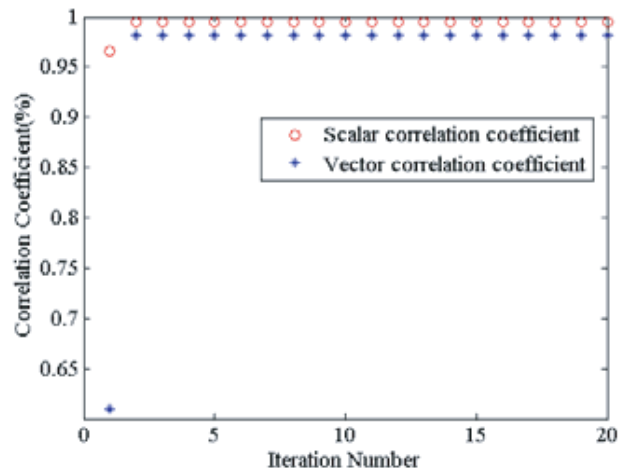


Figure 6. The variation of correlation coefficient with iteration numbers.

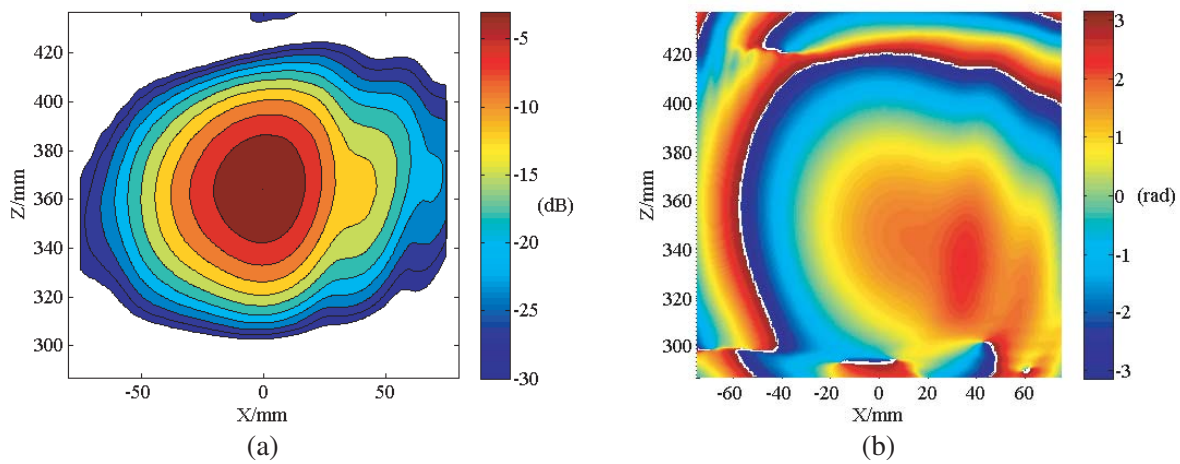


Figure 7. (a) Field amplitude (dB) distribution (b) phase pattern distribution on the window before phase-correcting.

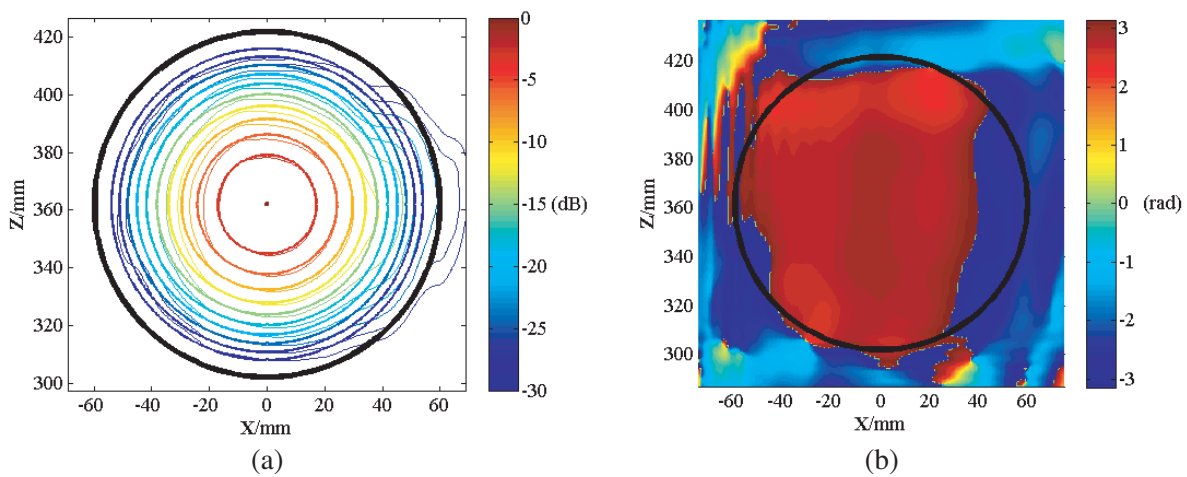


Figure 8. (a) Field amplitude (dB) distribution (b) phase pattern distribution on the window after phase-correcting.

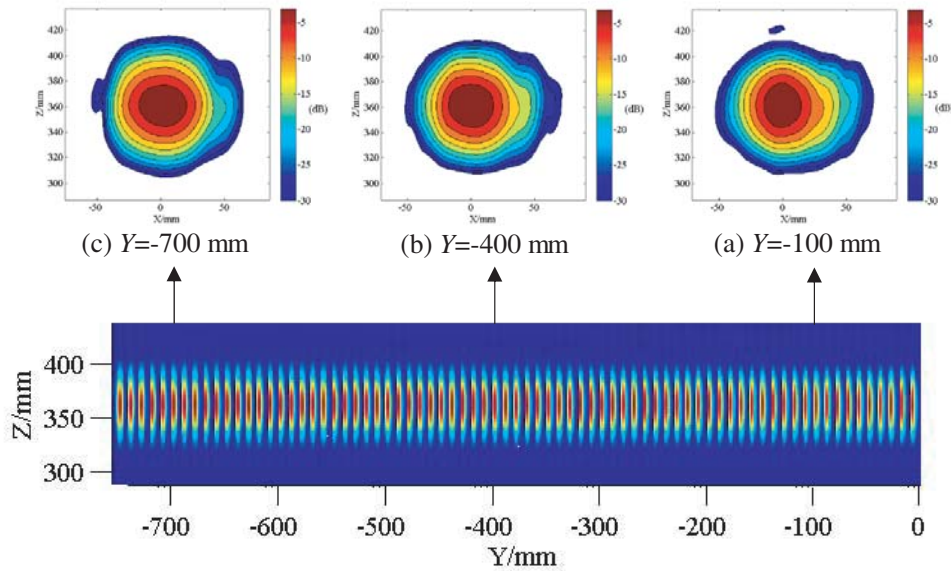


Figure 9. The radiation field of mirror 3 with KSA method.

contours is the field distribution radiated from mirror 3 after phase-correcting. The collected normalized power of this mirror system on the window is 0.9911, indicating that a transmission efficiency is 97.25%. Fig. 9 describes the radiation field of mirror 3, in which (a), (b), and (c) give the field distributions on the cross sections of $Y = -100$ mm, -400 mm, and -700 mm on the beam propagation axis, respectively. The beam does not diverge and has a good alignment property after reflected from mirror 3, which is still kept after a long distance of propagation.

4. PD METHOD TO DESIGN MIRROR SYSTEM

For the wave beam radiated from the launcher, astigmatism and ellipticity of the beams cannot be well corrected by those mirrors designed as toroidal, ellipsoidal, and paraboloidal surfaces. Besides adding a phase-correcting mirror after the bifocal mirror to reduce ellipticity and astigmatism, as introduced in Section 3, PD method can also be adopted [6, 17–19].

The parameters of the required beam can be obtained by:

$$\begin{cases} w_{m2} = w_{0out} \sqrt{1 + \left(\frac{2(y_{m2} - y_{0out})}{kw_{0out}^2} \right)^2} \\ w_{m3} = w_{0out} \sqrt{1 + \left(\frac{2(y_{m3} - y_{0out})}{kw_{0out}^2} \right)^2} \end{cases} \quad (6)$$

Table 2. Parameters of the mirror system designed by PD method.

	Mirror center (x_0, y_0, z_0) [mm]	Mirror size (dx, dz) [mm]	Focal length F_x [mm]	Focal length F_z [mm]	Tilt angle θ_x [deg]	Tilt angle θ_z [deg]
M1	(0, 60, 0)	(160, 70)	425	Inf	9.5	0
M2	(0, -330, 171.9)	(150, 150)	-	-	0	0
M3	(0, 100, 372.4)	(150, 150)	-	-	0	-11.5
Window	(0, -340, 372.4)	(60, 6)	Inf	Inf	0	0

where k is the wave number; w_{m2} is the beam radius on mirror 2 which is calculated from the beam radiated from mirror 1; w_{m3} is the beam radius on mirror 3 which is calculated from the ideal Gaussian beam on the window; y_{m2} and y_{m3} are the positions of mirror 2 and mirror 3, respectively; w_{0out} and y_{0out} are the waist radius and waist position of the required beam respectively. Assuming $y_{m2} = 0$ the solutions to Equation (6) are as follows [6]

$$\left\{ \begin{array}{l} w_{0out} = \sqrt{\frac{-B \pm \sqrt{B^2 - 4A(w_{m3}^2 - w_{m2}^2)}}{2A}} \\ A = F^2(w_{m3}^2 - w_{m2}^2) + 4F \\ B = -2F(w_{m3}^2 + w_{m2}^2) \\ F = \frac{k^2(w_{m3}^2 - w_{m2}^2)}{4L_{23}^2} \\ y_{0out} = -\frac{L_{23}}{\pm \sqrt{\frac{w_{m3}^2 - w_{0out}^2}{w_{m2}^2 - w_{0out}^2} - 1}} \end{array} \right. \quad (7)$$

where A , B , and F are the factors introduced during the process of solving Equation (6). L_{23} is the distance of mirror 2 from mirror 3. With respect to the different parameters in the X and Z directions, Equation (6) should be solved in the two perpendicular directions. The surface equation of mirror 2 can be written as follows [6]:

$$S(x, y, z) = \frac{\Delta\phi_{out} - \Delta\phi_{in}}{2k \cos \beta} \quad (8)$$

with $\Delta\phi_{out} = \phi_{out} - \phi_{cout}$, $\Delta\phi_{in} = \phi_{in} - \phi_{cin}$.

where $S(x, y, z)$ is the surface position of mirror 2, β the incident angle of the beam on the mirror 2, ϕ_{out} the phase pattern of the required wave beam, ϕ_{cout} the phase center of ϕ_{out} , ϕ_{in} the phase distribution of the incident beam on the flat mirror 2, and ϕ_{cin} the phase center of ϕ_{in} . Same ways can be used to design mirror 3. Parameters of the mirrors are shown in Table 2. Initially, mirror 2 and mirror 3 are plane mirrors.

Figure 10 shows the surface profile which is S in Equation (5) and the section profile of mirror 2 designed with PD method. Similarly, the surface profile and section profile of mirror 3 are shown

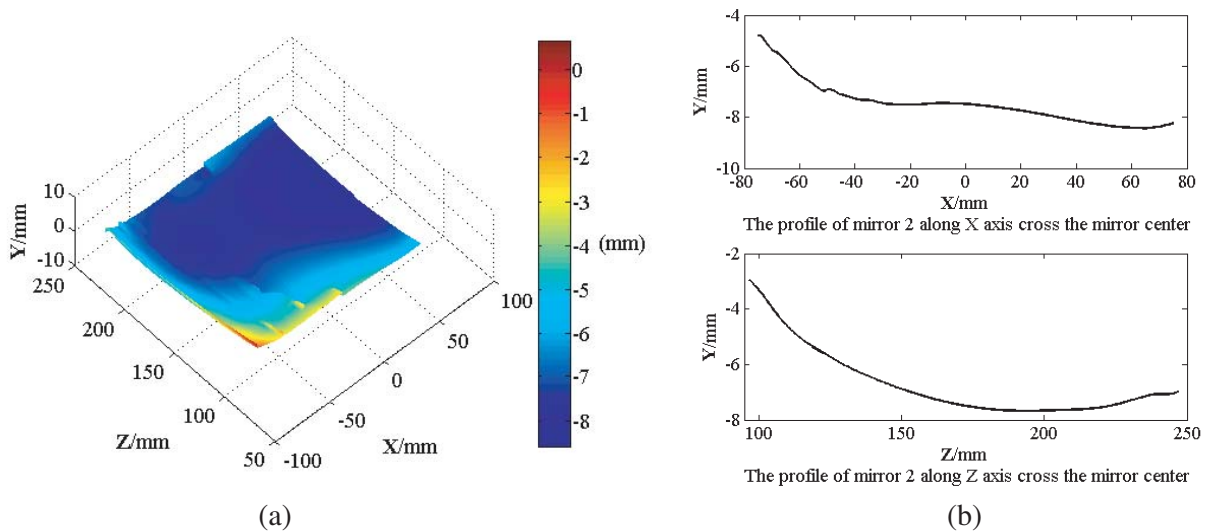


Figure 10. The (a) surface profile and the (b) section profile of mirror 2.

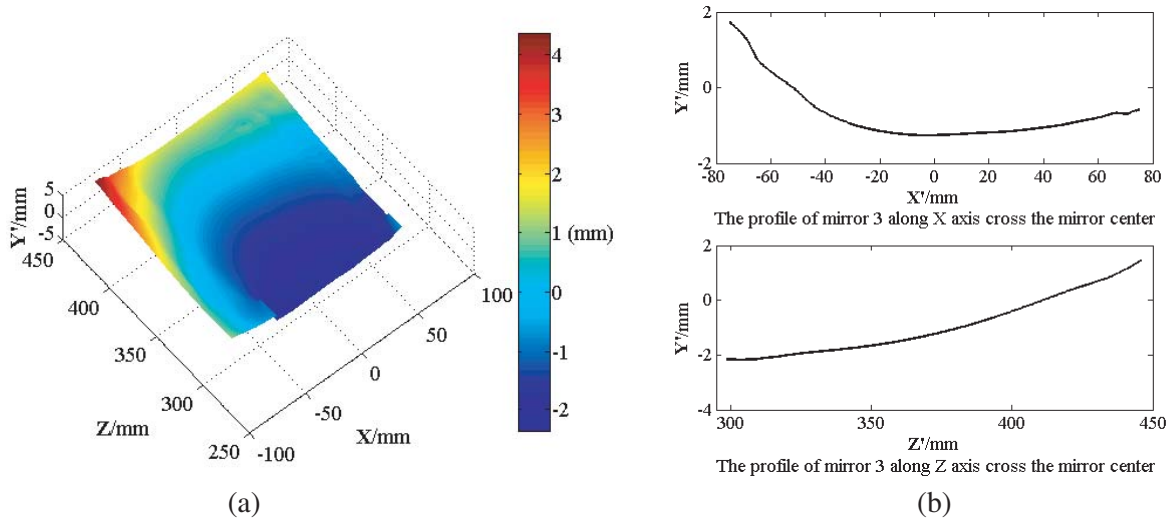


Figure 11. The (a) surface profile and the (b) section profile of mirror 3.

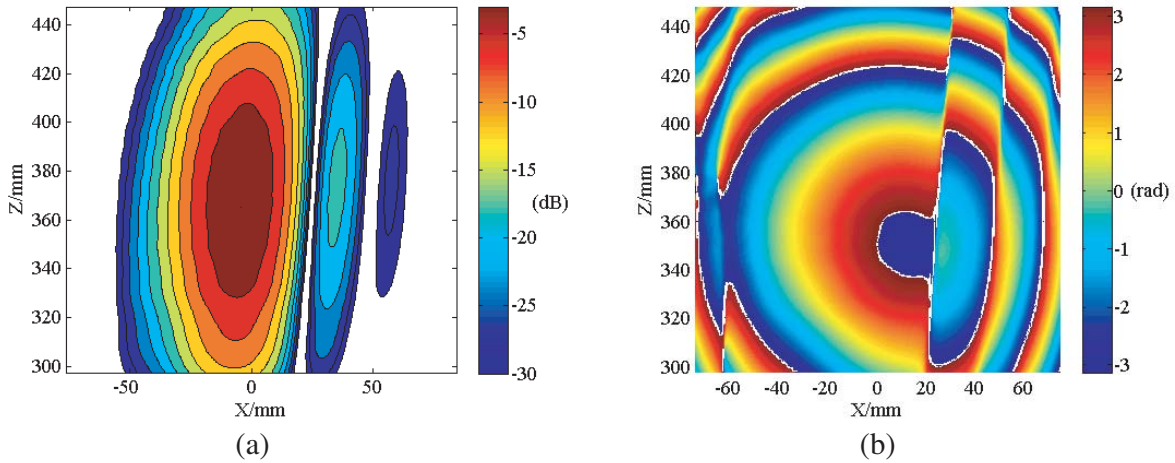


Figure 12. (a) Field amplitude (dB) distribution, (b) phase pattern distribution on the window before beam-shaping mirror design.

Table 3. Parameters of the input beam, the output beam and the ideal Gaussian beam in the mirror system.

Parameter	Incident beam	Output beam (KSA)	Output beam (PD)	Ideal Gaussian beam
Beam waist radius w_{0x} (mm)	50.07	28.56	28.40	29
Beam waist radius w_{0z} (mm)	32.95	28.85	28.97	29
Ellipticity	1.52	1.01	1.02	1
Astigmatism (mm)	500	50	0	0
η_s	0.919	0.9945	0.9973	1
η_v	0.6846	0.9812	0.9885	1

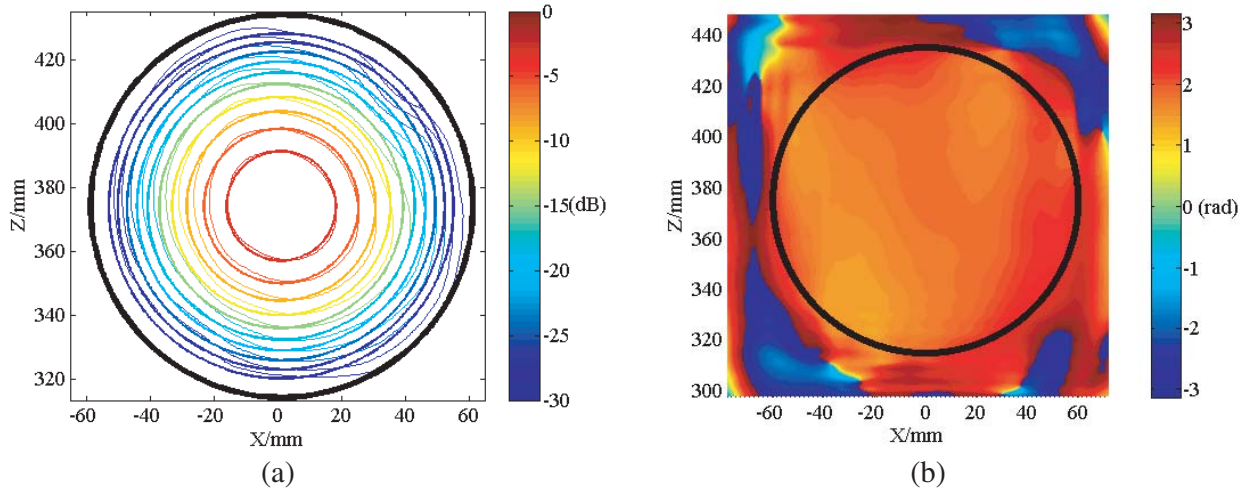


Figure 13. (a) Field amplitude (dB) distribution, (b) phase pattern distribution on the window after beam-shaping mirror design.

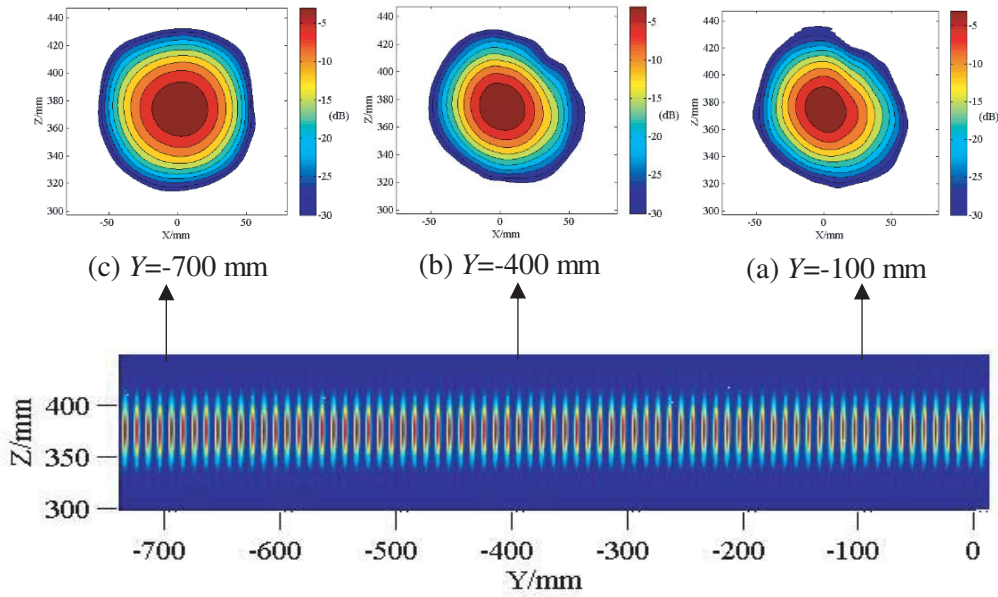


Figure 14. The radiation field of mirror 3 for PD method.

in Fig. 11(a) and Fig. 11(b), respectively. The field amplitude (dB) distribution and phase pattern distribution on the window before beam-shaping mirror design are shown in Fig. 12. Fig. 13 represents the field amplitude (dB) distribution and phase pattern distribution on the window after the design of the beam-shaping mirrors. In Fig. 13, the explanations of the black circle, thick contours, and thin contours can be found in Fig. 8. The scalar correlation coefficient and vector correlation coefficient are 99.73% and 98.85% respectively in Fig. 13(a). The window collects a normalized power of 0.9921 with a transmission efficiency of 97.67% for this mirror system. The radiation field of mirror 3 in this mirror system also has good alignment property. It focuses well and has no divergency (see Fig. 14).

5. DISCUSSION AND CONCLUSION

Table 3 shows the transformation of incident elliptical Gaussian beam by two mirror systems. The incident beam in Table 3 refers to the beam incident on the mirror 2. Both the KSA and PD methods can adjust the ellipticity and astigmatism of the incident beam. The results of adjusting ellipticity by the two methods are similar, while the result of adjusting astigmatism by PD method is better than KSA method. The vector Gaussian mode content on the window is above 98%, and the transmission efficiency achieves 97%, which greatly improves the efficiency of the quasi-optical mode converter.

Compared with PD method, the numerical simulation implementation of KSA method is simpler but more time-consuming because of the iterative calculation, especially in the design of mirror system with high frequency and large size. Generally, the iteration number of KSA method should not be less than 20 to achieve a converged result. For PD method, the design of the mirror system can be completed by solving Equation (6), and the scalar diffraction integral needs to be calculated only three times. It costs 17.01 minutes to design the mirror system using a computer with 16 GB memory and Intel Core i7 CPU at 3.4 GHz with PD method. However, the KSA method takes 131 minutes.

Therefore, KSA method is more suitable for the design of a small-size mirror system at low frequency and low astigmatism incident beam. In comparison, PD method can be applied more widely, but the mirror system designed by this method has two beam-shaping mirrors, which is more complicated than KSA method in practical implementation. An appropriate method should be chosen accordingly to design the mirror system.

REFERENCES

1. Tax, D. S., et al., "Experimental results on a 1.5 MW, 110 GHz gyrotron with a smooth mirror mode converter," *J. Infr. Millim. Terahertz Waves*, Vol. 32, No. 3, 358–370, 2011.
2. Zapevalov, V. E. and M. A. Moiseev, "Influence of aftercavity interaction on gyrotron efficiency," *Radiophysics and Quantum Electronics*, Vol. 47, 520–527, 2004.
3. Choi, E. M., M. A. Shapiro, J. R. Sirigiri, and R. J. Temkin, "Experimental observation of the effect of aftercavity interaction in a depressed collector gyrotron oscillator," *Physics of Plasmas*, Vol. 14, 093302, 2007.
4. Jin, J., M. Thumm, G. Gantenbein, and J. Jelonnek, "A numerical synthesis method for hybrid-type high-power gyrotron launchers," *IEEE Transactions on Microwave Theory and Techniques*, Vol. 65, No. 3, March 2017.
5. Wang, W., T. Song, H. Shen, S. Deng, D. Liu, and S. Liu, "Quasi-optical mode converter for a 0.42 THz TE_{17,4} mode pulsed gyrotron oscillator," *IEEE Transactions on Electron Devices*, Vol. 99, 1–5, 2017.
6. Jin, J., G. Gantenbein, J. Jelonnek, M. Thumm, and T. Rzesnicki, "A new method for synthesis of beam-shaping mirrors for off-axis incident Gaussian beams," *IEEE Transactions on Plasma Science*, Vol. 42, No. 5, 1380–1384, May 2014.
7. Murphy, J. A., "Distortion of a simple Gaussian beam on reflection from off-axis ellipsoidal mirrors," *International Journal of Infrared and Millimeter Waves*, Vol. 8, No. 9, 1165–1187, 1987.
8. Bogdashov, A. A., et al., "Mirror synthesis for gyrotron quasi-optical mode converters," *International Journal of Infrared and Millimeter Waves*, Vol. 16, No. 4, 735–744, 1995.
9. Perkins, M. P. and R. J. Vernon, "Two-dimensional phase unwrapping to help characterize an electromagnetic beam for quasi-optical mode converter design," *Appl. Opt.*, Vol. 47, No. 35, 6606–6614, 2008.
10. Katsenelenbaum, B. Z. and V. V. Semenov, "Synthesis of phase correctors shaping a specified field," *Radio Engineering Electronic Physics*, Vol. 12, 223–231, IEEE Press, New York, NY, USA, 1967.
11. Jin, J. B., B. Piosczyk, M. Thunmm, T. Rzesnicki, and S. C. Zhang, "Quasi-optical mode converter/mirror system for a high-power coaxial cavity gyrotron," *IEEE Transactions on Plasma Science*, Vol. 34, No. 4, 1508–1515, August 2006.

12. Bogdashov, A. A., A. V. Chirkov, G. G. Denisov, D. V. Vinogradov, A. N. Kuftin, V. I. Malygin, and V. E. Zapevalov, "Mirror synthesis for gyrotron quasi-optical mode converters," *International Journal of Infrared and Millimeter Waves*, Vol. 16, No. 4, 735–744, April 1995.
13. Yang, X., M. K. Thumm, A. Arnold, E. Borie, G. Dammertz, et al., "Progress toward optimization of phase-correcting mirrors for a multifrequency I-MW gyrotron," *IEEE Transactions on Plasma Science*, Vol. 34, No. 3, 652–658, 2006.
14. Jin, J., et al., "Design of phase correcting mirror system for coaxial-cavity ITER gyrotron," *Vacuum Electronics Conference IEEE*, 2010.
15. Liu, J., et al., "Design of adapted phase correcting mirrors for gyrotrons," *Vacuum Electronics Conference IEEE*, 2013.
16. Liu, J., et al., "Vector method for synthesis of adapted phase-correcting mirrors for gyrotron output couplers," *IEEE Transactions on Plasma Science*, Vol. 41, No. 9, 2489–2495, 2013.
17. Jin, J., et al., "High-efficiency quasi-optical mode converter for a 1-MW $TE_{32,9}$ -mode gyrotron," *IEEE Transactions on Plasma Science*, Vol. 41, No. 10, 2748–2753, 2013.
18. Dhakad, R. K., G. S. Baghel, M. V. Kartikeyan, and M. K. Thumm, "Output system for a 170-GHz/1.5-MW continuous wave gyrotron operating in the $TE_{28,12}$ mode," *IEEE Transactions on Plasma Science*, Vol. 43, No. 1, 391–397, January 2015.
19. Jin, J., G. Gantenbein, J. Jelonnek, M. Thumm, S. Alberti, J.-P. Hogge, M. Silva, and T. Goodman, "Quasi-optical mode converter for 1 MW dual frequency gyrotrons," *2017 Eighteenth International Vacuum Electronics Conference (IVEC)*, 1–2, 2017.